JOURNAL OF THEORETICAL
AND APPLIED MECHANICS
63, 3, pp. 701–710, Warsaw 2025
https://doi.org/10.15632/jtam-pl/208250

MONITORING OF STRUCTURAL STIFFNESS DEGRADATION AND IMPACT DAMAGE DETECTION BY CARBON FIBER SENSORS

Nikola SCHMIDOVÁ, Milan RŮŽIČKA, Karel DOUBRAVA, David BLAHA

Department of Mechanics, Biomechanics and Mechatronics, Faculty of Mechanical Engineering, Czech Technical University in Prague, Prague, Czech Republic

*corresponding author, *nikola.schmidova@cvut.cz*

This paper presents findings on the sensing capabilities of carbon fiber sensors (CFSs) for detecting impact damage in composite structures. New insights are provided into the correlation between stiffness degradation after impact and the measured response of integrated CFSs, placing both recent and previous data in a broader context. The results demonstrate the potential of CFSs for predicting structural stiffness loss and enabling effective impact damage monitoring. An experimental program focused on structural health monitoring (SHM) was carried out using CFSs embedded within flat specimens made of glass-fiber-reinforced polymer composites. The influence of cyclic loading on sensor response was investigated both before and after impact damage initiation during bending tests.

Keywords: carbon fiber sensor; SHM; electrical resistance; damage detection; composites.

1. Introduction

Long fiber reinforced polymer (FRP) composites are widely used in industries such as aerospace, automotive, manufacturing, and civil engineering. These materials are valued for their high strength, stiffness, low weight, and excellent resistance to fatigue. They are also used in infrastructure, such as bridges and roofs, where safety is critical. However, unlike traditional materials like steel, aluminum, or concrete, long FRP composites often fail without showing clear signs of damage. This makes it difficult to detect damage in time and highlights the need for advanced methods to monitor these materials.

Current inspections of FRP components often rely on scheduled visual checks, but these can easily miss hidden damage. While non-destructive testing (NDT) methods like C-scan, X-ray, thermography, and eddy current testing are more sensitive, they are time-consuming and usually require removing parts from service (Tabatabaeian *et al.*, 2022; Klute *et al.*, 2015; Gardiner, 2015; Kostroun & Dvořák, 2021). To overcome these challenges, structural health monitoring (SHM) systems are being developed. SHM allows for continuous monitoring of materials during use, providing real-time information about their condition. Originally developed for aerospace applications, SHM is now gaining attention in other industries to improve safety and reduce maintenance costs.

The publication has been funded by the Polish Ministry of Science and Higher Education under the Excellent Science II programme "Support for scientific conferences".
The content of this article was presented during the 40th Danubia-Adria Symposium on Advances in Experimental Mechanics, Gdańsk, Poland, September 24–27, 2024.

This work focuses on a specific method for SHM in FRP composites: the use of carbon fiber rovings for damage detection. This method takes advantage of the electrical properties of carbon fibers, which are conductive and piezoresistive. This means that their electrical resistance changes when they are stressed. These properties have been extensively studied, and different types of carbon fibers (e.g., PAN-based, graphite) are known to exhibit different levels of resistivity and piezoresistive behavior (Horoschenkoff & Christner, 2012; Wang & Chung, 1997; Scholle & Sinapius, 2021; Blazewicz *et al.*, 1997). Since individual carbon fibers are very thin (about 7–8 μm in diameter) and difficult to handle, bundles of fibers, called rovings, are often used instead. These rovings can contain thousands of fibers (e.g., 1 K, 3 K or 12 K), which makes them more practical for applications, but also introduces complexities in stress distribution and conductivity (Huang *et al.*, 2012; Huang & Wu, 2012).

For carbon fiber rovings to work as sensors, it is essential that good electrical contacts are prepared. Ideally, all fibers in the roving should contribute to the electrical signal. Poor contact can lead to inaccuracies caused by transverse resistance (Schulte & Baron, 1989). Methods to improve contact include the use of conductive paints, adhesives, metal splices or nickel coatings (Häntzsche *et al.*, 2013; Kalashnyk *et al.*, 2017; Gajda, 1978). The arrangement of these sensors is also important. They can be organized in simple meshes (Horoschenkoff & Christner, 2012) or in more complex arrangements (Park & Roh, 2021; Kunadt *et al.*, 2010) in which several rovings work together.

This study summarizes investigations regarding carbon fiber rovings to act as self-sensing materials for impact damage detection. Carbon fiber sensors (CFSs) can be successfully used as strain sensors. The sensors can be used as integrated sensors within a composite laminate, or they can be attached to the surface. It was shown that CFSs can be utilized also for impact damage detection (Schmidová *et al.*, 2018; 2022; 2023; 2024). CFSs were embedded in glass fiber composite plates. The sensors response to cyclic loading in the pristine state and after impact is described.

For practical applications, it would be beneficial to use longer sensors to monitor a larger area. For this reason, the influence of the length of the sensors on the possibility of impact damage detection using CFSs was also investigated.

The study also examined whether the amount of damage and the structural response could be predicted from the change in electrical resistance measured by CFSs.

Consider a beam of a manipulator with a working head drive. Different working heads with different masses move within the beam. We need to consider the variable loading of the beam. During the operation of the manipulator, a collision can occur, potentially reducing the beam's maximum load capacity due to damage. The detection of such collisions and the prediction of the residual strength of the structure would be useful.

A summary of current knowledge should contribute to the development of reliable and cost-effective SHM solutions.

2. Experimental campaign

Three experimental campaigns were conducted to evaluate the suitability of CFSs for impact damage detection, which provides a solid foundation for further applications:

- campaign 1: initial feasibility (Schmidová *et al.*, 2018);
- campaign 2: investigation of sensor positioning within the composite layup (Schmidová *et al.*, 2022);
- campaign 3: study of sensor length and correlation between sensor response and structural post-impact behavior (Schmidová *et al.*, 2023; 2024).

The basic evaluation of the individual experimental campaigns has been published in articles: (Schmidová *et al.*, 2018; 2022; 2023; 2024). In this paper, we analyze the relationships and

interconnections among the individual experimental campaigns. The comparison of the change in electrical resistance after impact for different lengths of CFSs will follow as well as detailed discussion regarding correlation between stiffness degradation after impact and the measured response of integrated CFSs.

2.1. Materials and specimen preparation

In the first experimental campaign, hand lamination was used for specimen preparation. The specimens were composed of two unidirectional layers of glass non-crimp fabric oriented in the [0]2 lay-up. CFSs were placed on one side of the fabric before curing. In the second and third experimental campaigns, specimens were manufactured using autoclave technology from prepreg sheets used in the aerospace industry. A $[+45/0/-45/90]_{\mathrm{sym}}$ laminate lay-up was used for the specimens. The specimens with integrated CFSs underwent the curing process: 125 °C for 90 minutes under the pressure of 6 bar.

Specimens were fabricated using glass fiber reinforced polymers and glass woven fabric prepregs. CFSs made from various types of carbon fiber rovings, including PAN-based and pitch-based fibers, were embedded within the specimens. Specimens underwent curing and were cut into strips for mechanical testing. Sensor integration and electrical connections were meticulously prepared to ensure reliable measurements.

2.2. Carbon fiber sensors

The CFSs were prepared from different carbon fiber rovings, see Table 1. The same methodology of CFS manufacturing was used as described in (Horoschenkoff & Christner, 2012). The ends of each roving were coated with a nickel electrolyte. A thin copper wire was then used to make electrical connections, as shown in Fig. 1.

Table 1. Overview of carbon fiber rovings used for CFS preparation.

	A	B	C	D	70A	95A
Label of the fiber [–]	T300 1000–50A	HTS40 A23 12K 1420TEX MC	HTS 40 MC	CN-80-30S	YSH-70A-30A	YSH-95A-30A
Type [–]	EX-PAN	EX-PAN	EX-PAN	EX-PITCH	EX-PITCH	EX-PITCH
Producer	Toray	Toho Tenax	Toho Tenax	Nippon Graphite Fibre Corporation		
Number of filaments used [–]	1000	7720	6000	3000	3000	3000
Metalization [–]	–	Nickel	–	–	–	–
E [GPa]	230	215	230	780	714	693
Elongation at break [%]	1.5	1.28	1.3	0.5	0.5	0.3

2.3. Mechanical loading – bending test

In all the experimental campaigns, the specimens were subjected to cyclic bending tests, followed by impact loading, and subsequently to cyclic bending tests again. In the first and second experimental campaigns, the specimens underwent three-point bending tests. In the third experimental campaign, a four-point bending (4PB) test was adopted, see Fig. 2. Switching the loading configuration from 3PB to 4PB resulted in a larger area of constant deformation under maximal loading. During all the tests, the maximum loading parameter corresponded to a maximum strain of 3.000 µm/m in the area of maximal loading.

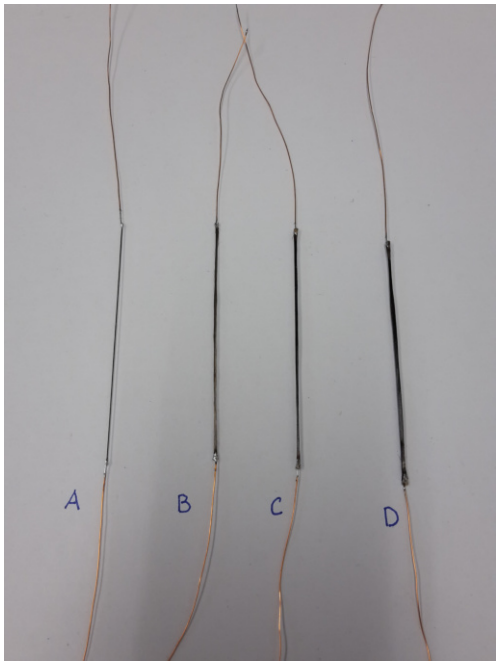

Fig. 1. CFSs prepared from different materials according to Table 1.

(a) 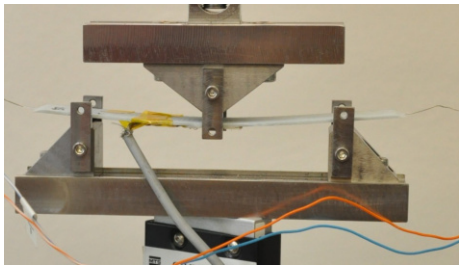 (b) 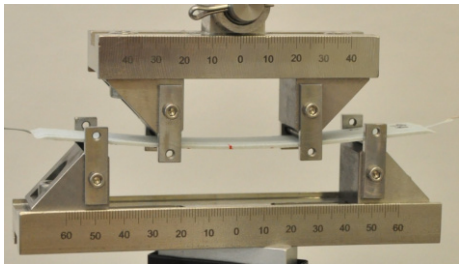

Fig. 2. Configuration of (a) three-point bending cyclic mechanical test during experimental campaign 1 and (b) four-point bending test cyclic mechanical test during experimental campaign 2.

2.4. Impact testing

Impact damage was induced using a drop weight impactor with energies ranging from 2 J to 4 J. An impactor with the diameter of 16 mm with the weight of 410 g was used. Electrical resistance measurements were recorded before and after impact loading to assess sensor performance. The impact energy of 2 J resulted in barely visible impact damage (BVID), see Fig. 3.

(a) 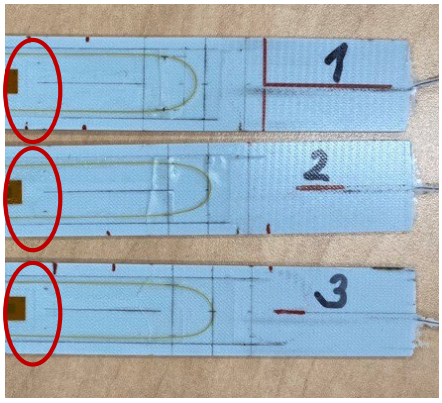 (b) 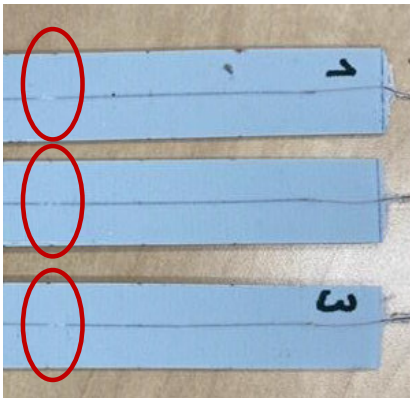

Fig. 3. Specimens from experimental campaign 3 after 2 J impact. CFSs are made of carbon fiber roving A (see Table 1) with the length equal to 140 mm. An impacted side (mold side of the specimen) in the section (a), bottom side of the specimen (b). The red circle indicates the impacted area.

In the third experimental campaign, three specimens were impacted also by the energy of 3 J and one specimen by the energy of 4 J. The energy of 4 J resulted in a crack of the specimen.

3. Results and discussion

Test results of each experimental campaign have added new information regarding sensing capabilities of CFSs. For the further usage of CFSs, this paper aims to put the information gained in greater context.

In the first experimental campaign, it was shown that CFSs are sensitive to impact damage detection. Cyclic mechanical loading causes the biggest difference in measured electrical resistance change to the most brittle material. On the other hand, the least brittle material showed the most stable behavior regarding cyclic loading.

The second experimental campaign included more specimens to broaden the statistics and to investigate the influence of positioning of the sensor within the lay-up. In the second experimental campaign, it was shown that brittle materials are much more difficult to handle during sensors preparation and even though they are more sensitive to impact damage, due to the difficulties associated with handling brittle fibers they are currently not suitable for further research. It was shown that thermographic inspection is suitable for CFSs integrated in glass reinforced composites and can serve for localization of the impact within the sensor's length. The CFSs response to temperature was described in the range of temperature levels 20 °C to 120 °C. It was revealed for all types of CFSs that the best position for impact damage detection within the lay-up is close to the opposite site to the impact and close to the impacted side.

In the third experimental campaign, CFSs made of Toray T300 1000-50A material were investigated, see Table 1. They were integrated between the 7th and 8th layer of the composite lay-up opposite to the impacted side of the specimen. The specimens were prepared using the same material and autoclave curing technology as during the second experimental campaign, but the length of the sensors was set to 140 mm.

During this experimental campaign, extensive cyclic testing was performed. Three specimens were first subjected to 1000 loading cycles, followed by a 2 J impact. Subsequently, the specimens underwent additional 1000 loading cycles. The increase in the number of loading cycles showed stable behavior of the sensor even for 1000 loading cycles, see Fig. 4. The relative electrical resistance change of the CFSs during cyclic loading was calculated according to Eq. (3.1), $R_{\text{max (loading CYCLE X)}}$ is equal to maximal electrical resistance of the CFS measured during the loading cycle, $R_{\text{min loading (CYCLE X)}}$ is equal to minimal electrical resistance measured during the loading cycle, $R_{\text{after implementation}}$ is equal to electrical resistance of the integrated CFS measured after implementation to the specimen:

$$\frac{\Delta R}{R} = \frac{R_{\text{max (loading CYCLE X)}} - R_{\text{min loading (CYCLE X)}}}{R_{\text{after implementation}}} \cdot 100\,[\%]. \tag{3.1}$$

The change in measured relative electrical resistance change of the sensor during cyclic loading before and after impact loading is more than 300 %. It is important to note that the size of the impact was so small that there were no signs of damage on the impacted side of the specimen, see Fig. 3a. According to this observation, it should be possible to detect impact damage of the CFS during scheduled inspections of the composite structure, which is necessary in many applications.

Because the same material for specimen preparation was used in the second and the third experimental campaign, it is possible to compare the response of sensors with the length of 70 mm and 140 mm, see Fig. 5. The analysis shows that the absolute changes in electrical resistance were identical for both sensor lengths. However, this indicates that the relative change in resistance is smaller for the longer sensors.

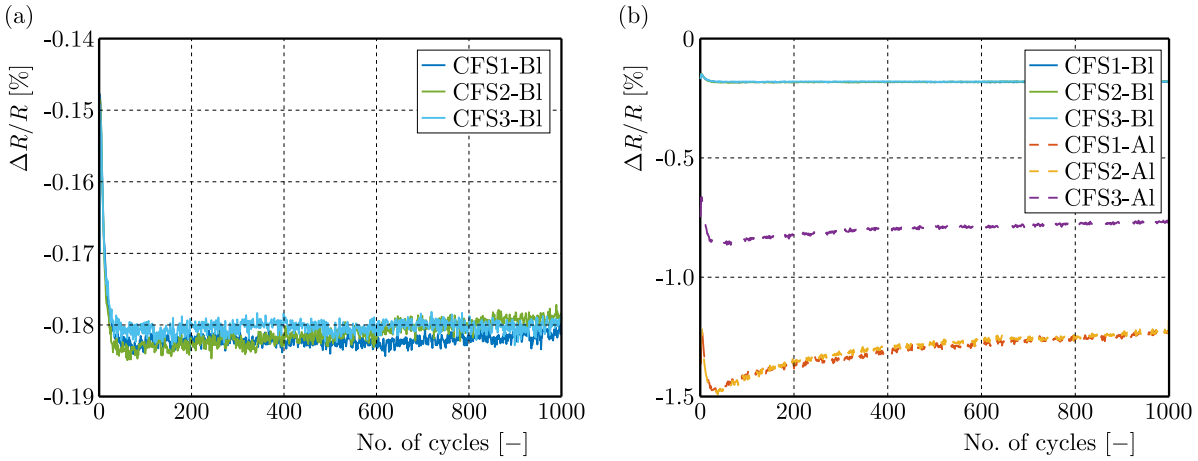

Fig. 4. Relative electrical resistance of the CFSs during cyclic test: (a) before impact (BI) for specimens CFS1, CFS2, and CFS3; (b) BI loading and after impact (AI) loading.

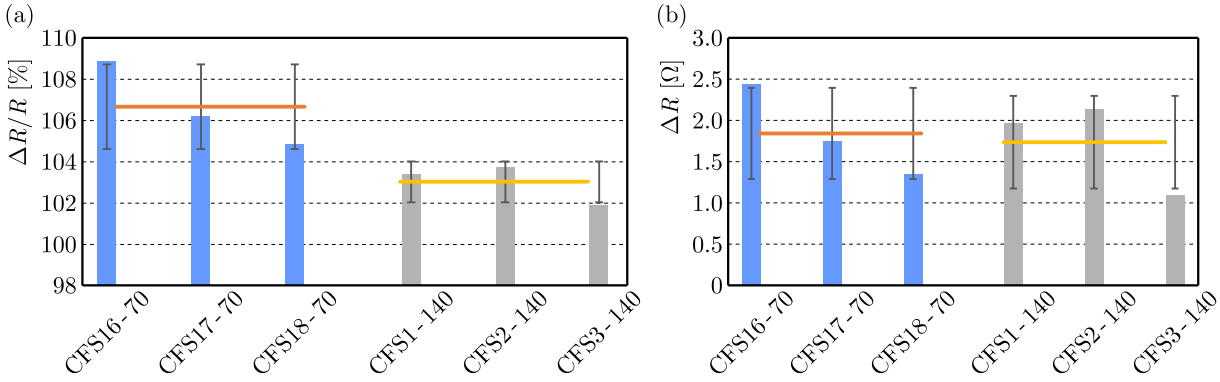

Fig. 5. (a) Relative electrical resistance change after BVID impact of 2 J of sensors with length of 70 mm and 140 mm; (b) absolute values of electrical resistance change of integrated CFS after BVID impact of 2 J.

This comparison enables better insight into the measurement preparation for more complex applications. When designing an application involving longer CFSs, it is necessary to consider the increased requirements for the measuring equipment, as it will be necessary to measure higher nominal resistance values. At the same time, the system must be capable of detecting small changes in electrical resistance resulting from impact events. Figure 6 shows extrapolated data for different possible lengths of CFSs up to the length of 1000 mm.

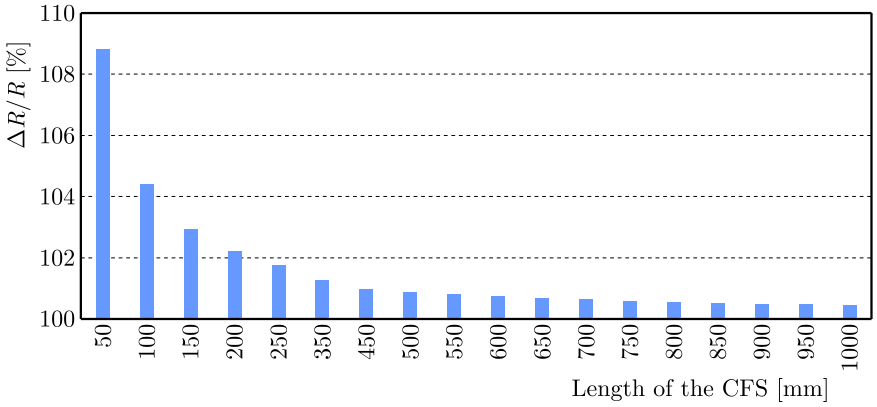

Fig. 6. Extrapolated relative electrical resistance change after BVID impact of 2 J for sensors with length from 50 mm to 1000 mm.

3.1. Correlation between stiffness degradation after impact and response of integrated CFSs

Furthermore, in the third experimental campaign, the change in measured electrical resistance during mechanical loading was investigated as a function of displacement of the specimen and force applied to the specimen before and after impact loading. These experimental data have not yet been presented in their full complexity; therefore, detailed information is provided here.

Figures 7 and 8 present the changes in the measured electrical resistance of the integrated CFSs in specimens exposed to different levels of impact loading (0 J, 2 J, 3 J, and 4 J). Following the impact loading, the specimens were subjected to four-point bending (4PB) tests.

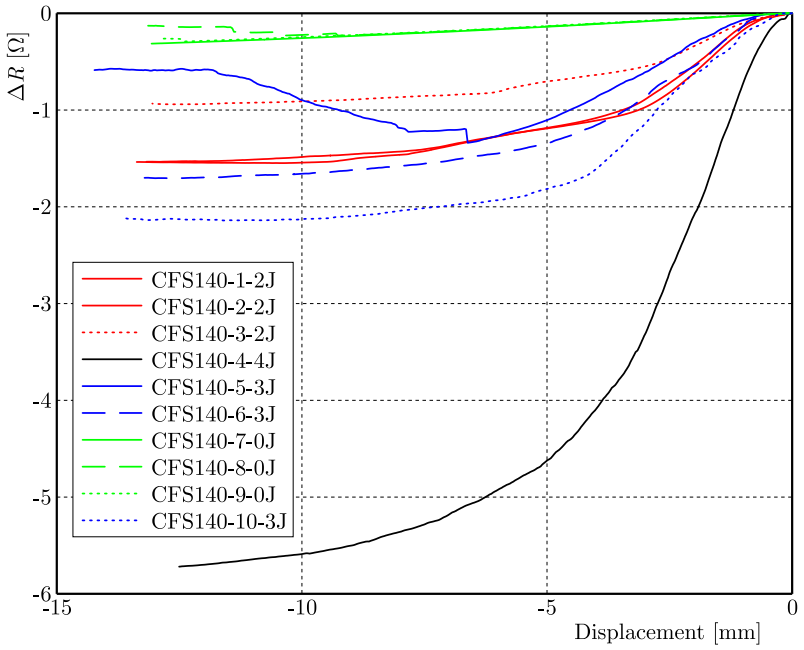

Fig. 7. Change of electrical resistance of the integrated CFS depending on applied displacement during 4PB.

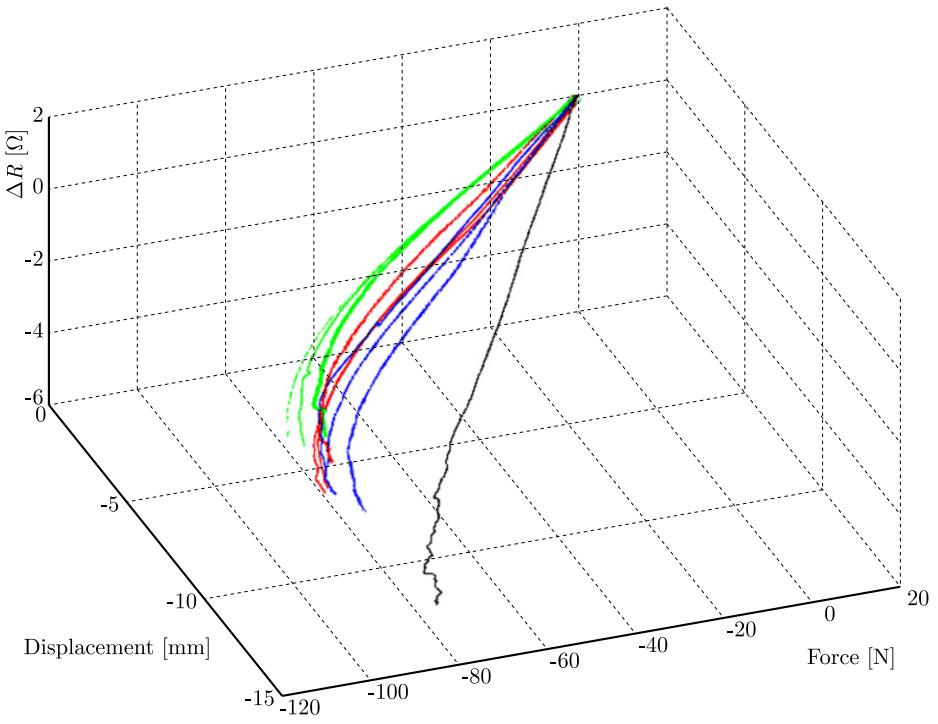

Fig. 8. 3D force-displacement-ΔR from integrated CFS during 4PB test.

The initial plan was to load the specimens until the final rupture; however, they proved to be too flexible. Despite setting the loading span to 20 mm and the support span length to 70 mm to achieve the maximum bending moment, only the specimen impacted with 4 J ultimately failed.

The configuration of the 4PB test was selected so that the applied loading force in both types of 4PB tests (loading/support spans of 20 mm/70 mm for the static test and 50 mm/100 mm for the cyclic test) produced equivalent bending moments and, consequently, the same strain levels. The loading limits for the cyclic tests were set to achieve a maximum strain of 3000 µm/m. This strain corresponds to a loading force of 30 N and a displacement of 2.65 mm.

Figure 7 shows data of the change in measured electrical resistance for each specimen, which was calculated according to the equation:

$$\Delta R = R_{\text{at the beginning of loading (deflection = 0 mm)}} - R_{(\text{deflection}=x\,\text{mm})}. \tag{3.2}$$

According to the 3D graph showing the relationship between ΔR, deflection, and force in Fig. 8, greater deflection amplifies the effect of stiffness loss caused by impact damage. The influence of increasing impact energy is relatively minor when comparing specimens impacted with 2 J and 3 J. However, the increase in impact energy from 3 J to 4 J results in a significant effect. This is likely due to the presence of different damage mechanisms in the specimen impacted with 4 J.

As shown in Fig. 7 and Fig. 8, it is difficult to distinguish between 2 J and 3 J impacts based on the data from the tested specimens alone. However, when comparing the measured data across all specimens (no impact, 2 J, 3 J, and 4 J impacts), there is a clear correlation between reduced stiffness (lower force required for the same level of deflection) and greater changes in the electrical resistance of the CFS induced by the impact. Specifically, higher impact energies result in lower forces required for the same displacement of the sensor and greater changes in the measured electrical resistance during loading.

Figures 7 and 8 also show that the relationship between the observed quantities is not uniform across the load range. Two distinct areas of slope can be identified in the load curve and a transitional area.

Figure 9 demonstrates that the decrease in the force required to achieve a defined displacement of the specimen (or structure) can be predicted both from the change in electrical resistance measured during loading and from the resistance change recorded before and after impact on the unloaded structure. The measured data provides a basis for predicting the structural behavior following impact events. Although the specimens were not loaded to complete fracture, it can be inferred that the force necessary to cause final failure correlates with both the impact energy and the magnitude of the measured change in electrical resistance of the integrated CFSs.

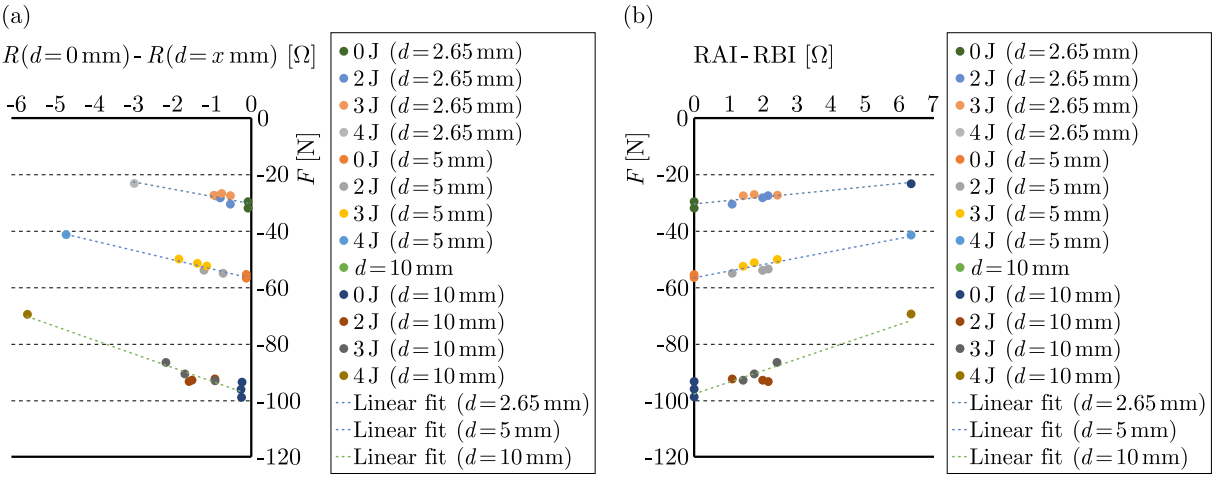

Fig. 9. Graph of force – change of measured electrical resistance for different impact energies and displacements (a) during loading ($d = x$ mm); (b) AI and BI.

4. Conclusions

Experimental measurements have been made using CFSs integrated into the glass composite. They showed that CFSs are promising tools for impact damage detection in composite structures.

A recommendation regarding the material used for carbon fiber roving in sensor preparation was made. The influence of temperature change and cyclic mechanical loading on the measured signal was described. It was shown that thermographic inspection can be used for the inspection of CFSs and for closer focusing of the impact position within the length of the sensor, also applicable for BVID.

The change in electrical resistance of CFSs after impact loading at identical energy levels is comparable, even for sensors twice the length. This suggests that longer sensors are suitable for detecting small impact damage, facilitating the mapping of impact events over larger component areas.

CFSs show stable responses to cyclic mechanical loading, with consistent $\Delta R/R$ values observed for all three sensors tested. Following impact loading, the sensor response increases significantly during subsequent loading, with measured $\Delta R/R$ values more than three times greater than those recorded prior to impact.

The results indicate that impact damage in a structure subjected to specific loading cycles can be detected by measuring the sensor response during operational shutdowns.

A strong correlation was found between the change in electrical resistance of the integrated CFSs and the reduction in stiffness of the specimens caused by impact loading. This relationship allows for the prediction of stiffness reduction in the structure using two different approaches:

– by measuring the change in electrical resistance of the built-in sensors during load cycles;

– by comparing the electrical resistance of the sensors before and after the impact.

These results highlight the potential of CFSs for monitoring impact damage and predicting the loss of structural stiffness, providing valuable tools for assessing the condition of in-service components.

Acknowledgments

This work has been supported by project No. FW06010296 of the Technological Agency of the Czech Republic.

References

1. Blazewicz, S., Patalita, B., & Touzain, Ph. (1997). Study of piezoresistance effect in carbon fibers. *Carbon*, *35*(10–11), 1613–1618. https://doi.org/10.1016/S0008-6223(97)00120-6

2. Gajda, W.J. (1978). *A fundamental study of the electromagnetic properties of advanced composite materials*. https://api.semanticscholar.org/CorpusID:136838814

3. Gardiner, G. (2015). Structural health monitoring: NDT-integrated aerostructures. *Composites World*. https://www.compositesworld.com/articles/structural-health-monitoring-ndt-integrated-aerostructures-enter-service

4. Häntzsche, E., Matthes, A., Nocke, A., & Cherif, Ch. (2013). Characteristics of carbon fiber based strain sensors for structural-health monitoring of textile-reinforced thermoplastic composites depending on the textile technological integration process. *Sensors and Actuators A: Physical*, *203*, 189–203. https://doi.org/10.1016/j.sna.2013.08.045

5. Horoschenkoff, A., & Christner, C. (2012). Carbon fibre sensor: Theory and application. In N. Hu (Ed.), *Composites and Their Applications* (pp. 219–242). InTech. https://doi.org/10.5772/50504

6. Huang, H., & Wu, Z.S. (2012a). Static and dynamic measurement of low-level strains with carbon fibers. *Sensors and Actuators A: Physical*, *183*, 140–147. https://doi.org/10.1016/j.sna.2012.06.006

7. Huang, H., Yang, C., & Wu, Z. (2012b). Electrical sensing properties of carbon fiber reinforced plastic strips for detecting low-level strains. *Smart Materials and Structures*, *21*(3), Article 035013. https://doi.org/10.1088/0964-1726/21/3/035013

8. Kalashnyk, N., Faulques, E., Schjødt-Thomsen, J., Jensen, L.R., Rauhe, J.C.M., & Pyrz, R. (2017). Monitoring self-sensing damage of multiple carbon fiber composites using piezoresistivity. *Synthetic Metals*, *224*, 56–62. https://doi.org/10.1016/j.synthmet.2016.12.021

9. Klute, S.M., Metrey, D.R., Garg, N., & Rahim, N.A.A. (2015). In-situ structural health monitoring of composite-overwrapped pressure vessels. *Luna Innovations Incorporated*. Retrieved June 5, 2023, from https://lunainc.com/sites/default/files/assets/files/resource-library/36_Klute_2015_Luna_InSituSHM_COPV_final.pdf

10. Kostroun, T., & Dvořák, M. (2021). Application of the pulse infrared thermography method for nondestructive evaluation of composite aircraft adhesive joints. *Materials*, *14*(3), Article 533. https://doi.org/10.3390/ma14030533

11. Kunadt, A., Heinig, A., Starke, E., Pfeifer, G., Cherif, C., & Fischer, W.-J. (2010). Design and properties of a sensor network embedded in thin fiber-reinforced composites. In *2010 IEEE Sensors* (pp. 673–677). https://doi.org/10.1109/ICSENS.2010.5690085

12. Park, Y.-B., & Roh, H.D. (2021). Electromechanical analysis of CFRP for real-time structural self-sensing and non-destructive evaluation. In *Nondestructive Characterization and Monitoring of Advanced Materials, Aerospace, Civil Infrastructure, and Transportation XV* (Article 11710). SPIE. https://doi.org/10.1117/12.2582669

13. Schmidová, N. (2024). *Electrical resistance measurement for structural health monitoring of composite materials* [Doctoral dissertation, Czech Technical University in Prague, Faculty of Mechanical Engineering].

14. Schmidová, N., Horoschenkoff, A., & Růžička, M. (2018). Investigation of the electrical resistivity of damaged carbon fibers sensors with regard to SHM. In *Proceedings of the ECCM18*. https://www.academia.edu/69240591/Investigation_of_the_Electrical_Resistivity_of_Damaged_Carbon_Fibers_Sensors_with_Regard_to_SHM

15. Schmidová, N., Macken, J., Horoschenkoff, A., Sedláček, R., Kostroun, T., Šimota, J., & Růžička, M. (2022). Impact damage detection of a glass fabric composite using carbon fiber sensors with regard to mechanical loading. *Applied Sciences*, *12*(3), Article 1112. https://doi.org/10.3390/app12031112

16. Schmidová, N., Sedláček, R., Kratochvíl, A., & Růžička, M. (2023). Behavior of carbon fiber sensors under cyclic loading and impact damage. In *Proceedings of the 33rd Workshop of Applied Mechanics* (pp. 1–3). Czech Technical University in Prague, Faculty of Mechanical Engineering.

17. Scholle, P., & Sinapius, M. (2021). A review on the usage of continuous carbon fibers for piezoresistive self strain sensing fiber reinforced plastics. *Journal of Composites Science*, *5*(4), Article 96. https://doi.org/10.3390/jcs5040096

18. Schulte, K., & Baron, C. (1989). Load and failure analyses of CFRP laminates by means of electrical resistivity measurements. *Composites Science and Technology*, *36*(1), 63–76. https://doi.org/10.1016/0266-3538(89)90016-X

19. Tabatabaeian, A., Liu, S., Harrison, P., Schlangen, E., & Fotouhi, M. (2022). A review on self-reporting mechanochromic composites: An emerging technology for structural health monitoring. *Composites Part A: Applied Science and Manufacturing*, *163*, Article 107236. https://doi.org/10.1016/j.compositesa.2022.107236

20. Wang, X., & Chung, D.D.L. (1997). Electromechanical behavior of carbon fiber. *Carbon*, *35*(5), 706–709. https://doi.org/10.1016/S0008-6223(97)86644-4

Manuscript received December 15, 2024; accepted for publication July 14, 2025; published online July 22, 2025.